Anal. Chem. **2002,** *74,* 3470−3475

A Chip System for Size Separation of Macromolecules and Particles by Hydrodynamic Chromatography

Emil Chmela and Robert Tijssen*

Department of Chemical Engineering, University of Amsterdam, Nieuwe Achtergracht 166, 1018 WV, Amsterdam, The Netherlands

Marko T. Blom, Han J. G. E. Gardeniers, and Albert van den Berg

MESA Institute, University of Twente, The Netherlands, PO Box 217, 7500 AE Enschede, The Netherlands

For the first time, a miniaturized hydrodynamic chromatography chip system has been developed and tested on separation of fluorescent nanospheres and macromolecules. The device can be applied to size characterization of synthetic polymers, biopolymers, and particles, as an attractive alternative to the classical separation methods such as size exclusion chromatography or field-flow fractionation. The main advantages are fast analysis, high separation efficiency, negligible solvent consumption, and easy temperature control. The prototype chip contains a rectangular flat separation channel with dimensions of 1 μm deep and 1000 μm wide, integrated with a 300-pL injector on a silicon substrate. The silicon microtechnology provides precisely defined geometry, high rigidity, and compatibility with organic solvents or high temperature. All flows are pressure driven, and a specific injection system is employed to avoid excessive sample loading times, demonstrating an alternative way of lab-on-a-chip design. Separations obtained in 3 min show the high performance of the device and are also the first demonstration of flat channel hydrodynamic chromatography in practice.

Size characterization of synthetic polymers, biopolymers, and particles becomes one of the main issues in today's analytical chemistry. Although optical techniques such as light scattering (LS) or direct microscope measurements can be used, separation methods such as size exclusion chromatography (SEC) or flow and thermal field-flow fractionation (FFFF and ThFFF) offer the easiest and simplest way to size characterization including size distribution. However, despite the overall improvement in separation methods for low molecular weight compounds, which involves notably miniaturization, separations of large (noncharged) species are still performed in a rather old-fashioned way with use of large columns and detectors, high consumption of (often) toxic solvents, low efficiency, and rather long analysis times. In the case of ThFFF, also high electrical power consumption is at hand.

Hydrodynamic chromatography (HDC),[1−10] provides faster and more efficient analysis than the previously mentioned methods as it is based on the effect of the flow profile on an analyte carried through a tube of comparable size and does not involve slow mass transfer. However, here also, classical instrumentation partly limits the performance due to extracolumn peak broadening, when realized in columns packed with nonporous particles, especially for packing particle sizes below 3 μm.[10]

Undoubtedly all the named polymer separation methods should profit from miniaturization. One possibility is using packed or open capillaries. Here, size exclusion electrochromatography (SEEC)[11] seems promising but electroosmosis in some organic solvents used for synthetic polymers is inherently small or not stable enough, which prevents its universal application. Moreover, packing of capillaries is still a difficult task, also making pressure-driven miniaturized SEC difficult to utilize. Another novel approach is hollow fiber flow field-flow fractionation (HF5), recently realized in our group.[12] HDC has been successfully performed even in 1-μm-i.d. capillaries; however, detection turned out to be rather difficult,[6,7] because of the short absorption length, i.e., the capillary internal diameter.

Another miniaturization approach is based on the progress in silicon-based microtechnology in recent years, aiming toward micro total analysis systems (μTAS)[13] as initiated by the pioneering work of Terry in 1979 and illustrated more recently. Since then, most research in this field was devoted to electrophoretic chips, especially for genomics and proteomics.[14] In contrast, very little progress has been made toward pressure-driven liquid chroma-

* Corresponding author: (e-mail) rtijssen@science.uva.nl; (fax) +31 20 525 5604; (phone) +31 20 525 6550.

(1) Pedersen, K. O. *Arch. Biochem. Biophys. Suppl.* **1962**, *1*, 157−168.
(2) DiMarzio, E. A.; Guttman, C. M. *Macromol.* **1970**, *3*, 131−146. DiMarzio, E. A.; Guttman, C. M *J. Polym. Sci. B* **1969**, *7*, 267−272.
(3) Small, H. *J. Colloid Interface Sci.* **1974**, *48*, 147−161.
(4) Small, H.; Saunders, F. L.; Solc, J. *Adv. Colloid Interface Sci.* **1976**, *6*, 237−266.
(5) Brenner, H.; Gaydos, L. J. *J. Colloid Interface Sci.* **1977**, *58*, 312−356.
(6) Tijssen, R.; Bos, J.; van Kreveld, M. E. *Anal. Chem.* **1986**, *58*, 3036−3044.
(7) Bos, J.; Tijssen, R.; van Kreveld, M. E. *Anal. Chem.* **1989**, *61*, 1318−1321.
(8) DosRasmos, J. G. In *Particle Size Distributions III, Assessment and Characterization*; Provder, Th., Ed.; ACS Symposium Series 693; American Chemical Society: Washington, DC, 1998; pp 207−221.
(9) Prieve, D. C.; Hoysan, P. M. *J. Colloid Interface Sci.* **1978**, *64*, 201−213.
(10) Venema, E.; Kraak, J. C.; Poppe, H.; Tijssen, R. *J. Chromatogr., A* **1996**, *740*, 159−167.
(11) Kok, W. T.; Stol, R.; Tijssen, R. *Anal. Chem.* **2000**, *72*, 468A−476A.
(12) van Bruijnsvoort, M.; Kok, W. Th.; Tijssen, R. *Anal. Chem.* **2001**, *73*, 4736−4742.
(13) van den Berg, A.; Lammerink, T. S. J. *Topics Curr. Chem.* **1997**, *194*, 21−50.

10.1021/ac0256078 CCC: $22.00
Published on Web 06/06/2002

tography on a chip and consequently also in such separation methods for large noncharged species. The main reason seems to be the absence of suitable micropumps, existing only as prototypes.[15] The alternative of applying electroosmosis[16] is problematic for many organic solvents. The latter also cause problems with glued capillaries used mostly as inlet and outlet connections. The first LC chip device by Manz[17] dates back to 1990. In 1995, Ocvirk[18] from the same group performed some separations but the efficiency was very limited. Only recently, Kutter,[19] Ericson,[20] and McEnery[21] have presented more promising results. Despite another fruitful approach called shear-driven chromatography (SDC) by Desmet,[22] the need for pressure-driven chip systems remains.

So far, the only chip devices for separation of noncharged large species are microfluidic dielectrophoretic FFF (DEP-FFF)[23] and microfluidic ThFFF,[24] suitable for a limited group of analytes.

The crucial problem in chip systems still seems to be the detection because of the very small sample volumes. One possibility to increase detection sensitivity would be the use of extreme aspect ratio channels where the large width ensures more analyte loadability while shallow depth is needed to preserve efficiency or in the case of HDC also selectivity. This larger width would only serve detection in a side-in fashion. However, the large cross section does improve the possibilities for integrated off-column detection techniques. This could for instance consist of a deeper and narrower optical slit at the end of the separation channel. Apart from recent exceptions,[21,22,25] there is no practical experience with channels of (sub)micrometer depth and large aspect ratios.

In this paper, we present a novel on-chip HDC system consisting of an extremely shallow, large aspect ratio separation channel (1 μm deep and 1000 μm wide) with integrated injection, fabricated using silicon and glass microtechnology. The main advantages would be fast analysis, high separation efficiency because of microfluidic integration, negligible solvent consumption, and potentially easy temperature control due to the shallow depth. Silicon microtechnology[26] should provide the required almost perfect geometry, rigidity, and compatibility with organic solvents or high temperature. In the field of microdetectors, developments are still going on, so a prototype without an integrated detector was fabricated for tests with fluorescently labeled materials using FIM imaging. Although, in this case, straightforward fluorescence detection in the shallow channel is used, which does not profit from a wider channel, the device is designed using a width that is as large as possible. The reason for this is that the fabrication of such a wide, shallow channel is a technological challenge,[27] which could influence the separation performance itself. Observation of possible peak distortion in such channels would assist the future integration of microdetectors. Further reducing the channel depth should also allow a new separation mechanism for polymers by chain reptation[28] as proposed by Tijssen[29] in 1992.

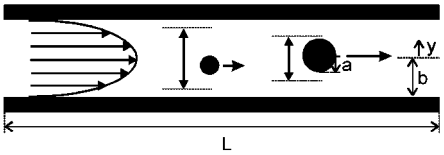

Figure 1. Principle of HDC separation. Larger analytes cannot sample low fluid velocities near the channel wall and therefore move faster.

THEORY

Basic Principle. In narrow conduits (effective size ≤ 1 μm) with a laminar flow (Figure 1), larger molecules or particles (size range from 0.002 to 0.2 of the conduit size) are transported faster than smaller ones as they cannot fully access slow-flow regions near the conduit walls.[4,6] In HDC, this is used for analytical separation in applications similar to traditional size exclusion chromatography (SEC). The separation effect occurs in packed columns or open microcapillaries and, as demonstrated here, also in flat microchannels.

Flat Channel Fluidics. Pressure-driven laminar flow in channels with rectangular cross sections has been described analytically.[30] For channels with a large aspect ratio, say >10, the flow velocity is practically uniform over the channel width except near the edges, while having a parabolic profile over the shorter dimension. The system can be approximated by infinite planeparallel plates separated by a distance equal to the channel height. The velocity profile over the channel height and the pressure drop over its length are then[30]

$$u(y) = {}^3/_2\langle u\rangle\left[1 - (y/b)^2\right] \quad (1)$$

$$\Delta p = \frac{3\eta L\langle u\rangle}{b^2} \quad (2)$$

Here, $\langle u\rangle$ is the average velocity of the fluid, y the vertical distance form the central plane in the channel, b half of the channel thickness, L the channel length and η the dynamic viscosity of the fluid.

(14) Harrison, D. J., van den Berg, A., Eds. *Proceedings μTAS '98 Conference*; Kluwer Academic Publishers: Dordrecht, The Netherlands, 1998. van den Berg, A., Olthuis, W., Bergveld, P., Eds. *Proceedings μTAS '00 Conference*; Kluwer Academic Publishers: Dordrecht, The Netherlands, 2000.
(15) van Lintel, H.; et al. *Sens. Actuators* **1988**, *15*, 153−167.
(16) Schasfoort, R. B. M.; Schlautmann, S.; Hendrikse, J.; van den Berg, A. *Science* **1999**, *286*, 942−945.
(17) Manz, A.; Miyahara, Y.; Miura, J.; Watanabe, Y.; Miyagi, H.; Sato, K. *Sens. Actuators, B* **1990**, *1*, 249−258.
(18) Ocvirk, G.; Verpoorte, E.; Manz, A.; Grasserbauer, M.; Widmer, H. M. *Anal. Methods Instrum.* **1995**, *2*, 74−82.
(19) Kutter, J. P.; Jacobson, J. C.; Matsubara, M.; Ramsey, J. M. *Anal. Chem.* **1998**, *70*, 3291−3297.
(20) Ericson, C.; Holm, J.; Ericson, T.; Hjertén, S. *Anal. Chem.* **2000**, *72*, 81−87.
(21) McEnery, M.; Tan, A.; Alderman, J.; Patterson, J.; O'Mathuna, S. C.; Glennon, J. D. *Analyst* **2000**, *125*, 25−27.
(22) Desmet, G.; Baron, G. V. *Anal. Chem.* **2000**, *72*, 2160−2165.
(23) Wang, X.; Yang, J.; Huang, Y.; Vykoukal, J.; Becker, F. F.; Gascoyne, P. R. C. *Anal. Chem.* **2000**, *72*, 832−839.
(24) Edwards, T. L.; Gale, B. K.; Frazier, A. B. *Anal. Chem.* **2002**, *74* (6), 1211−1216. Edwards, T. L.; Gale, B. K.; Frazier, A. B. Proc. 1999 BMES/EMBS Conf., Atlanta, GA, 1999; p 848.
(25) Han, J.; Craighead, H. C. *Science* **2000**, *288*, 1026−1029.
(26) Fintschenko, Y.; van den Berg, A. *J. Chromatogr., A* **1998**, *819*, 3−12.
(27) Blom, M. T.; Chmela, E.; Gardeniers, J. G. E.; Tijssen, R.; van den Berg, A. *Sens. Actuators, B* **2002**, *82*, 111−116.
(28) Casassa, E. F. *J. Phys. Chem.* **1971**, *75*, 3929−3939.
(29) Tijssen, R. In *Theoretical Advances in Chromatography and Related Separation Techniques*; Dondi, F., Guiochon, G., Eds.; Kluwer Academic Publishers: Dordrecht, The Netherlands, 1992; pp 397−441.
(30) Batchelor, G. K. *An Introduction to Fluid Dynamics*; Cambridge University Press: London, 1991.

Retention. In HDC, the retention behavior has been described by several models, the simplest taking into account only geometrical effects. The more extended models by DiMarzio and Guttman[2] and Brenner and Gaydos[5] can be unified for all HDC geometries to obtain the calibration relationship between residence time and size:

$$\tau = (1 + B\lambda - C\lambda^2)^{-1} \tag{3}$$

Here τ is the relative retention time and λ the relative size of the analyte with respect to the channel. These quantities are defined as $\tau = t_R/t_0$ (where t_0 is the time of elution of a small compound) and $\lambda = a/b$ if a is a properly chosen analyte radius (for a hard sphere, a is its geometrical radius) and b the radius of a capillary or half of the thickness of a flat channel. Constants B and C are both geometry dependent; constant C is also model dependent. Constant B represents directly the effective "cutoff" of the parabolic flow profile for an analyte at the inner boundary of the wall-adjacent layer from which this analyte is excluded and thus reflects the main retention mechanism of HDC. Flat rectangular channels can be accurately described by planeparallel plates for the case of retention, resulting in $B = 1$. In circular cylindrical and polygonal cross sections $B = 2$ [unpublished theoretical study in cooperation with Dr. H. Hoefsloot (UvA)]. The constant C accounts for the fact that large particles slightly lag the virtual local velocity of the fluid in their center of mass. This slip velocity is caused by the curvature of the flow profile and also by the rotation−translation coupling as the particles are forced to rotate by a force couple stemming from different fluid velocities at opposite sides. DiMarzio and Guttman[2] found for planeparallel plates that $C = (1/2) + (3/4)\gamma$, γ being a function of the particle shape and density distribution $\gamma = 2\pi/27$ for free-draining polymer coils and $\gamma = 2/3$ for impermeable hard spheres. Thus the HDC calibration eq 3 becomes

$$\tau = (1 + \lambda - 0.68\lambda^2)^{-1} \quad \text{(flat channel; polymers)} \tag{3a}$$

$$\tau = (1 + \lambda - \lambda^2)^{-1} \quad \text{(flat channel; particles)} \tag{3b}$$

However, those authors neglect the hydrodynamic interaction of a sphere moving close to a wall, which increases the value of the C constant substantially as was pointed out by Brenner and Gaydos.[5] They present a corrected approximation for a cylindrical tube but no explicit result for a planar geometry. Furthermore, the above formulas do not reflect radial forces such as the hydrodynamic "tubular pinch" effect,[29,31] which occurs at higher velocities, and electrostatic and electrokinetic lift forces acting upon charged particles in mainly aqueous solutions.[32] Those forces change the uniformity of the concentration profile of the particles over the channel cross section, thus favoring certain velocities and influencing the retention. With all the effects included, the retention curve especially for colloids is more complicated than eq 3, as was described by Tijssen.[29] This is also apparent from experimental results of Small,[3] and Noel interpreted by Ploehn,[31] the latter presenting trendlines with several inflex points.

(31) Ploehn, H. J. *Int. J. Multiphase Flow* **1987**, *13*, 773−784.
(32) Hollingsworth, A. D.; Silebi, C. A. In *Particle Size Distributions III, Assessment and Characterization*; Provder, Th., Ed.; ACS Symposium Series 693; American Chemical Society: Washington, DC, 1998; pp 244−265.

Peak Dispersion. Theoretical plate height in the case of planeparallel plates was derived by Golay,[33] who found for unretained compounds

$$H = \frac{2D}{\langle u \rangle} + \frac{4b^2}{105D}\langle u \rangle \tag{4}$$

where D is the diffusion coefficient of the analyte. For finite size solid particles D can be calculated from the Stokes−Einstein equation as

$$D = kT/6\pi\eta a \tag{5}$$

Equation 4 is analogous to the corresponding equation for a circular geometry. For unretained compounds, only the geometrical factor 4/105 replaces the factor 1/24 for circular tubes. This means that the efficiency is roughly similar for circular and planar channels. Assuming $D \sim 10^{-10}$ m^2/s for smaller analytes, channel depth 1 μm and length 8 cm, more than 100 000 plates should be obtained in HDC chip analysis.

In addition, the stagnant layers along the sides of the channel become important for dispersion as they retain some sample and the mass transfer over the wide channel is slow. Various studies of this phenomenon were performed, applying the same nonequilibrium theory as for the short dimension,[34−37] arriving at a rather disfavoring plate height contribution 8 times higher than the ideal plate height from eq 4. However, Doshi[38] and Dutta[39] considered the transient state, which applies in our case, i.e., when $D \sim w$ (w is the channel width), resulting in a much lower dispersion. Proper investigation of this phenomenon will be covered in our coming work, also using computational fluid dynamics (CFD) simulations.

It must be noted, however, that for larger analytes formula 4 also has to be corrected for their finite size. This has been performed by various authors;[2,5,40] their results, however, differ substantially. Our future experiments and revisions of the theory should reveal the correct expressions. Again, numerical simulations should be helpful in this.

EXPERIMENTAL SECTION

Chip Fabrication. The prototypes were fabricated by silicon and glass microtechnology. An optically polished 4-in. silicon wafer of 525-μm thickness (Silicon Valley Microelectronics Inc., San Jose, CA) was thermally oxidized to 1-μm depth, spin-coated with photoresist, and photolithographically patterned. The separation channel was created by wet silicon oxide etching, the inlet and outlet slits were by reactive ion etching. A 4-in. Pyrex glass wafer 500 μm thick (Corning, New York) was polished, and inlet and outlet holes of 0.5-mm diameter were created by powder blasting. The glass wafer was then directly bonded on top of the silicon

(33) Golay, M. J. E. In *Gas Chromatography*; Desty, D. H., Ed.; Butterworths: London, 1958.
(34) Giddings, J. C.; Schure, M. R. *Eng. Sci.* **1987**, *42*, 1471−1479.
(35) Takahashi, T.; Gill, W. N. *Chem. Eng. Commun.* **1980**, *5*, 367−385.
(36) Golay, M. J. E. *J. Chromatogr.* **1981**, *216*, 1−8.
(37) Cifuentes, A.; Poppe, H. *Chromatographia* **1994**, *39*, 391−404.
(38) Doshi, M. R.; Daiya, P. M.; Gill, W. N. *Chem. Eng. Sci.* **1978**, *33*, 795−804.
(39) Dutta, D.; Leighton, D. T., Jr. *Anal. Chem.* **2001**, *73*, 504−513.
(40) Giddings, J. C. *Sep. Sci. Technol.* **1978**, *13*, 241−254.

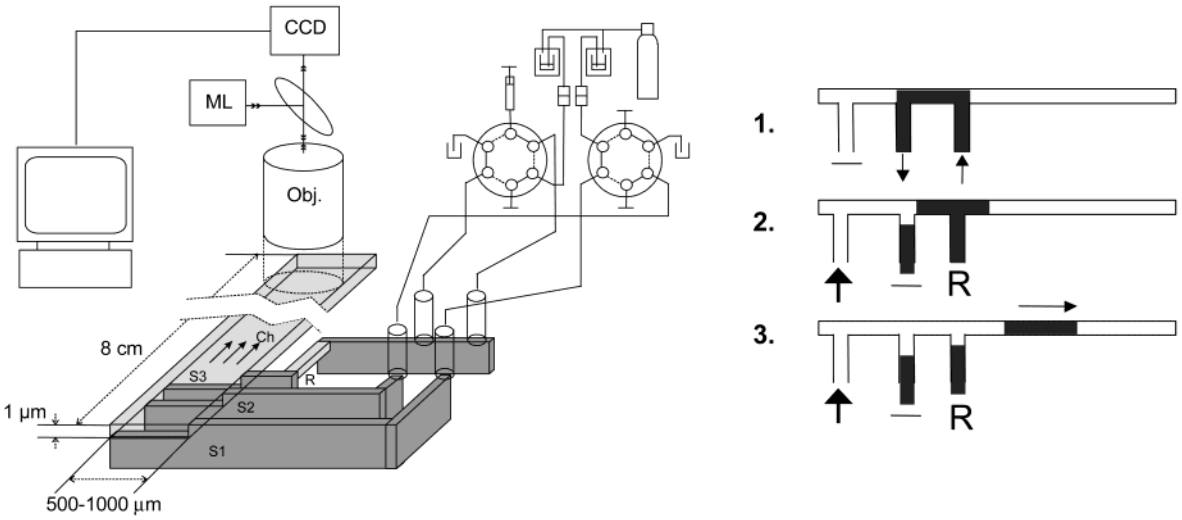

Figure 2. (a) Prototype experimental setup. The HDC chip (not to scale) contains a separation channel (Ch), a resistance channel (R), and inlet and outlet slits for sample (S2, S3) and carrier liquid (S1). The chip is connected to a valve flow-actuation system, solvent being pressed in from gas-pressurized vessels. An imaging microscope is used to view the separations. (b) Injection scheme in HDC chip. Sample is filled between the second and third slit (1). After switching the valves, the carrier liquid flow is set on, sweeping the sample plug out into the separation channel (2). Partial back-leak into the slits, controlled by the valve and resistance R prevents sample tailing (3).

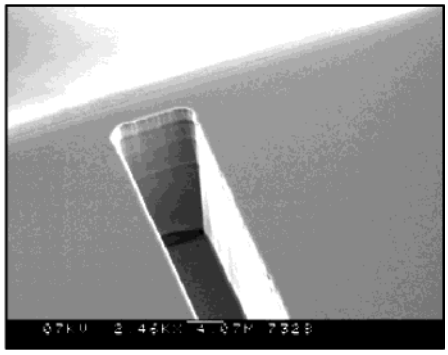

Figure 3. SEM picture of the injection slit and part of the separation channel.

wafer and annealed at 350 °C. The fabrication has been described in more detail in a previous paper.[27]

Apparatus. In the test setup (Figure 2a), prototype HDC chips were used containing an integrated flow-actuated subnanoliter-volume injector (Figure 2b, Figure 3) and the separation channel, which was 1 μm deep, 1 mm wide, and 80 mm long. The chip was clamped to a macroflow-actuating system, solvent being pressed in from gas-pressurized vessels. An upright fluorescence imaging microscope (BX51) equipped with a thermoelectrically cooled CCD camera (Colorview 12) and a computer image acquisition and processing system (Olympus, Zoetermeer, The Netherlands) was used with the prototypes to view the separations. The internal microscope mercury lamp (ML) served as illumination; in some experiments, an additional external light source, Efos Elite (Efos, Gent, Belgium), was used to increase the illumination intensity. All tubing and valves used were stainless steel standard HPLC $^{1}/_{16}$-in. components (Valco). A homemade clamp with a precisely machined stainless steel connection piece with grooves for O-rings was used as an interface between the chip top glass wafer with the inlet and outlet holes and the solvent system.

Chemicals. The particles used as test analytes were fluorescently labeled polystyrene latex nanoparticles Carboxylate Modified FluoroSpheres YellowGreen Fluorescent of nominal diameters 26, 44, and 110 nm, obtained from Molecular Probes (Leiden, The Netherlands). Fluorescein-labeled anionic dextran of (mass, 10 kDa) was obtained from the same provider. Fluorescein sodium salt was obtained from Acros Organics (Geel, Belgium).

The eluent contained 0.5 g/L Triton X100 as the nonionic surfactant (Acros Organics, Geel, Belgium) dissolved in 10 mM phosphate buffer, pH 7, with 2 mM sodium azide as the preservative. Sodium phosphate salts and sodium azide were obtained from Merck (Darmstad, Germany). All water used was deionized and subboil-distilled. The buffer was filtered prior to use through a 0.02-μm membrane filter. Upstream from each reservoir, a 0.5-μm in-line filter (Upchurch) was placed.

Procedures. The samples were prepared by dissolving fluorescein (0.05 mg/mL), the nanoparticles, and dextran (0.2−0.5 mg/mL) in the eluent, and the resultant mixture was sonicated before injection. Working pressure was in the range of 2−7 bar. The whole separation was recorded as a sequence of microscope images by moving the chip system on a micrometer translation stage.

Safety. Exposure to sodium azide has to be eliminated during the buffer preparation by working with gloves and under a hood because of its high toxicity. Waste solutions have to be diluted with water to prevent formation of explosives. When the external illumination UV source is used, UV glasses and protective nontransparent clothing and gloves have to be worn and highly inflammable materials removed form the reach of the light.

RESULTS AND DISCUSSION

Design and Technology. In the design of the chip, we have balanced chromatographic requirements and technological possibilities. The channel length is limited by the 4-in. Si wafer size to 8 cm, yet it should provide ~100 000 theoretical plates. In obtaining this, channel cross-section uniformity and well-defined depth of ~1 μm are crucial parameters. The channel height variations stemming from channel etching and from polishing and

bonding of the top wafer are in the order of few nanometers as well as the deformation caused by applied working pressure.

The optimum velocity estimated from minimum peak broadening (eq 4) is in the order of 0.1−1.0 mm/s, and thus, the working pressure from eq 2 should be 1−10 bar. However, future planned submicrometer channels would require much higher pressures. Therefore, we studied pressure limitations first. In a series of experiments and calculations, we found the maximum pressure before the chip bond breaks to be inversely proportional to the channel width squared.[41] For channels 0.5 mm wide, the maximum pressure was ~80 bar. Using this pressure limit and eqs 2 and 4, we can estimate the smallest channel depth in which we could achieve the optimum linear velocity with pressure-driven flow for $D = 1 \times 10^{-10}$ m^2 s^{-1} as 0.56 μm, the velocity being 2.5 mm/s. In smaller channels, the velocity has to be lower than the optimum, but even then, high efficiencies can still be achieved. For example in a 0.25-μm-thick channel of the same length where the maximum attainable linear velocity would be 0.5 mm/s, 200 000 plates would be achieved for the same compound, while the selectivity would be 4 times higher than in the 1-μm channel.

The connections of the solvent and sample inlet and outlet tubing turned out to be problematic when glued fused-silica capillaries were used, since all glues were eventually attacked by THF. Next, anodic bonding of a Kovar piece with soldered HPLC tubing was attempted on the top glass wafer.[42] However, residual stress caused cracks when connecting to the solvent actuator system. Therefore, we are now using clamped connections with chemically resistant O-rings instead. This design has proven to be very reliable.

In the injection system, the injection length, i.e., the spacing between slits 2 and 3, was chosen to be 300 μm, thus causing only a minor contribution to the peak dispersion. Common action of the valves and of the properly chosen resistances of the microchannels allows reproducible injection of a rectangular sample plug using only pressure-driven flows. CFD simulations were used extensively during the design and were later confirmed by the experiment. This work will be covered in a separate paper.

Separations. An example of the particle separation experiments is given in Figure 4. The separations achieved in 3 min (working pressure 4 bar) indicate the high performance of the device. Retention and efficiency data from this and two other experiments under the same conditions are summarized in Table 1. From the standard deviations, it is apparent that the precision of these preliminary data is limited. In the case of retention this is due to the low maximum acquisition rate (2 s^{-1}) of the imaging system and in the case of efficiency due to the low fluorescence intensity. In agreement with the HDC theory, larger particles are carried faster by the flow, 110-nm particles eluting first, followed by 44- and 26-nm particles, and finally small molecules. However, fluorescein seems to be much more separated from the other analytes (Figure 4B,G) than what simple HDC theory would predict. Likely, fluorescein is additionally delayed by interaction with the channel surface. This is also indicated by its larger zone dispersion caused by slow mass transfer between the surface and the eluent. We suppose the channel walls are negatively charged as both the glass and the partly oxidized silicon should have dissociative silanol groups on its surface in the pH 7 aqueous buffer. This should prevent the fluorescein anion from adsorption

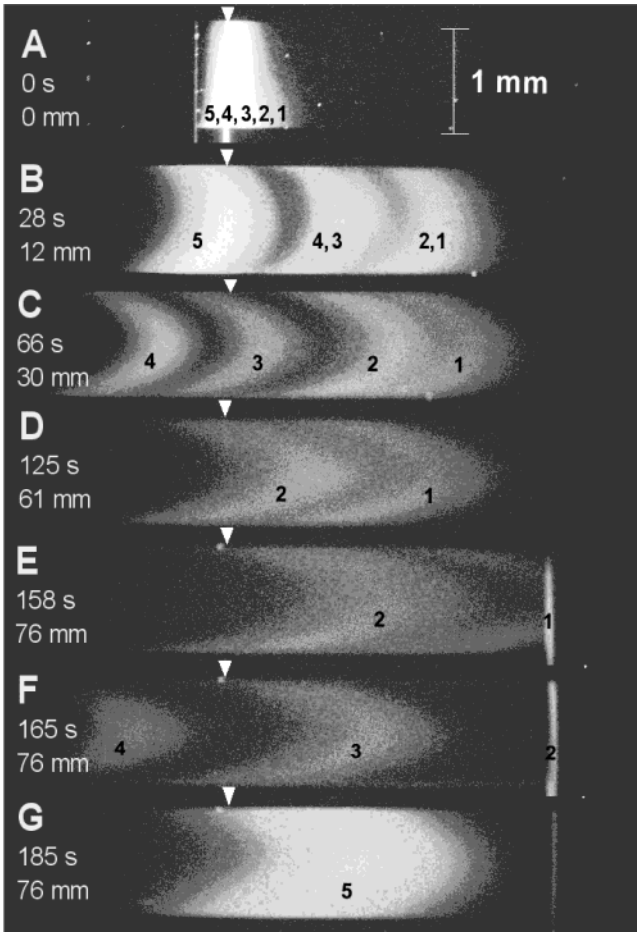

Figure 4. Separation on the HDC chip (top view) of fluorescein (0.05 mg/mL) (5), fluorescently labeled anionic dextran 10 kDa (4) as the marker, and fluorescent polystyrene particles of 26- (3), 44- (2), and 110-nm diameter (1); concentration 0.25−0.5 mg/mL in 10 mM phosphate buffer (pH 7.0); working pressure 4 bar. Flow is from the left to the right. The channel is 1 mm wide and 1 μm deep. After the mixture injection (A), fluorescein is separated first (B), and further downstream the dextran and the particles are resolved (C−G). Distance (arrow pointer) and the time passed since injection are indicated on the left. At the end (E−G) some of the zones are eluting already into the outlet slit, visible as a bright line on the right.

Table 1. Measured and Predicted Relative Retention and Efficiency at the Channel End in the HDC Chip Test Separations

	τ		N	
	experiment[a]	theory	experiment[a]	theory
fluorescein	1.096 ± 0.016	1.000	14 000 ± 2 000	36 000[b]
dextran 10 kDa	0.994[c]	0.994	31 000 ± 7 000	192 000
particles				
26 nm	0.957 ± 0.006	0.975	33 000 ± 3 000	252 000
44 nm	0.925 ± 0.005	0.960	20 000 ± 3 000	180 000
110 nm	0.900 ± 0.003	0.911	35 000 ± 42 000[d]	79 000

[a] Mean ± std; $n = 3$. [b] Assumed $D = 5 \times 10^{-10}$ m^2/s. [c] Theoretical value. [d] Two data points.

(41) Blom, M. T.; Tas, N. R.; Pandraud, G.; Chmela, E.; Gardeniers, J. G. E.; Tijssen, R.; Elwenspoek, M.; van den Berg, A. J. *Microelectromech. Syst.* **2001**, *10*, 158−163.

(42) Blom, M. T.; Chmela, E.; Gardeniers, J. G. E.; Berenschot, J. W.; Elwenspoek, M.; Tijssen, R.; van den Berg, A. J. *Micromech. Microeng.* **2001**, *11*, 382−385.

but is probably not strong enough to eliminate all interactions. Since excessive retention of fluorescein was observed in our previous experiments, we have tried to use a small fluorescently labeled anionic dextran as a marker instead. This polymer exists in solution as a random coil with ~6-nm diameter.[43] The theoretical retention of this molecule calculated from eq 3b is $\tau = 0.9941$, and all data are corrected for this value.

A different situation arises in the case of the particles. Those contain carboxylic groups on the surface and are thus considerably negatively charged. All dye material is intercalated inside the particle and does not have any influence on the particle surface properties as claimed by the manufacturer. However, all the particles seem to elute earlier than what eq 3a predicts. Although the dextran marker might also interact slightly with the surface and thus increase the apparent t_0, other effects should play a role because the deviations vary with the particle size. Particularly, the exclusion of 44-nm particles is excessive. At high ionic strengths, possible different surface properties e.g., charge surface charge densities, can play a role if particle−surface interactions occur when the compressed electrical double layer allows the particles to get closer to the channel surface.[9] However, nonmonotonic HDC curves have also been reported by Ploehn[31] even in much larger conduits, stemming from electrostatic, electrokinetic, and hydrodynamic lift forces. Despite the high ionic strength and low velocities we are using, these factors could partly act in our case too. Further experiments at various mobile-phase velocities and ionic strengths would be necessary to fully explore the retention behavior.

For polymer molecules, especially in organic solvents, less complicated behavior such as that observed in packed columns or microcapillary HDC is expected.

Efficiency. Integration of the fluorescent zones over the central part (10%) of the channel width has been performed to evaluate the efficiency in the number of theoretical plates N (Table 1). The low fluorescence intensity at the end of the separation channel has limited and, in one case, prevented the estimation. Roughly 15 000 plates were obtained for fluorescein and 20 000−40 000 plates for larger analytes.

Theoretical values of N in Table 1 are based on the plate height H obtained from eqs 4 and 5. Although the experimental performance is still high and sufficient for an HDC separation, it is notably lower than what the theory predicts. The central part of the zone may still be broadened by lateral mass transfer from its deformed sides. This clear crescent deformation of the zones apparently stems from a nonuniform flow profile over the channel width. We assume this is caused by mismatch in the thermal expansion coefficients of silicon and glass.[27] In cooling after direct bonding annealing both wafers slightly bend, one a little more than the other. This translates into increased channel thickness and thus enhanced flow speed in the middle of the channel. This zone deformation is different from the already mentioned side wall effect, which produces a different shape of the zone, more flat in the middle and with longer tails adjacent to the side.[39] This effect is present as well but is hidden in the larger dispersion caused by the nonuniform flow.

The partial integration results in higher apparent efficiency than if the whole channel width was used, but only such selected data should be compared to the theoretical values from eq 4. In practice, one could incorporate a split at the end of the channel to cut off the deformed zone sides and let only the center part enter a detector or, alternatively, incorporate splitting structures at the end to delay the central part of the peak. Besides, a narrower (but still wide enough) channel should be effected much less by the wafer deformation.[27]

CONCLUSIONS

For the first time, the feasibility of an HDC chip for fast size characterization of larger analytes has been demonstrated. The obtained results for separation of fluorescent nanoparticles correspond qualitatively to HDC theory, but the retention and dispersion models need improvement for a quantitative description. The observed excessive zone bending can be explained by residual mechanical stress in the microdevice and can be readily eliminated by reduction of the channel width. In the next stage, tests on polymer separation in organic solvents will be performed, whereas the integration of more sophisticated detectors will be undertaken.

ACKNOWLEDGMENT

The presented work is a part of the project 'Hydrodynamic Chromatography in Integrated Micromachined Separation Systems' carried out by cooperation of the University of Amsterdam and the University of Twente and funded by the Dutch Technology Foundation STW-NWO as Project AAC4556. Dr. H. Hoefsloot (UvA) is thanked for his derivations on the model constants B and C. The authors also thank A. Mank from Philips research laboratory for initial help on the imaging setup

Received for review March 1, 2002. Accepted April 29, 2002.

AC0256078

(43) Ioan, C. E.; Aberle, T.; Burchard, W. *Macromolecules* **2000**, *33*, 5730−5739.